growth arises when secular perturbations and gas drag act together to establish size-dependent encounter velocities that remain low when colliding bodies are of similar size. Collisions between bodies of markedly different size are at high velocity and can lead to cratering and erosion, but our simulations show that growth overcomes erosion (Fig. 2). This general result should apply regardless of whether the perturbations are from Jupiter-like companions formed earlier by disk instability, stellar-mass objects in multiple-star systems, or short-lived instabilities that lead to asymmetries in the massive protoplanetary disk. We propose classifying this new form of runaway growth as "Type II."

Classical "Type I" runaway growth occurs in a self-gravitating population of planetesimals. Random orbital kinetic energy is exchanged during gravitational encounters between large and small bodies, and the population trends toward energy equipartition, a process dubbed "dynamical friction" (*22*). Dynamical friction lowers the encounter velocities of the larger bodies with respect to each other, enhancing their effective collision cross-sections and increasing the rate at which they accumulate each other. Under these conditions, nearly the entire growth period up to embryo size is in Type I runaway mode. In our simulations, which are not self-gravitating, the size-dependent phasing of orbital elements holds encounter velocities low between all similar-size bodies (typically 1 to 10 m s^{-1}) (Fig. 1). Initially, these encounter velocities exceed the planetesimal escape velocities so there is no enhancement of collision cross sections and growth is orderly. As larger and larger bodies grow, their escape velocities approach and then exceed the relatively low encounter velocities, causing the transition from orderly growth to Type II runaway growth. In this way, the effects of dynamical friction are mimicked by the size-dependent phasing of orbital elements.

Our attempts at including self-gravitating planetesimals (*23*) indicate that when the distribution reaches 10^{24} to 10^{25} g the mutual perturbations are beginning to become important, although they are still dominated by the size-dependent phasing of secular perturbations. This suggests that just as Type II runaway is getting under way, the population may begin a transition to Type I runaway or evolve by some combination of the two. A more rigorous treatment using hardware and software capable of efficiently handling a very large number of self-gravitating bodies (*24*, *25*) could confirm this. The identification of Type II runaway growth suggests that planetary bodies can form in environments in which protoplanetary orbits may have higher eccentricities and inclinations than are usually considered. In addition to the Solar System model we provide here, other examples include young multiple-star systems and the post-supernova environment in binary-pulsar systems.

References and Notes

1. V. S. Safronov, *Evolution of the Protoplanetary Cloud and Formation of the Earth and Planets* (Nauka, Moscow, Russia, 1969) [translated for NASA and NSF by Israel Program for Scientific Translation, 1972; NASA TT F-677].
2. V. Mannings, A. P. Boss, S. S. Russell, Eds., *Protostars and Planets IV* (Univ. of Arizona, Tucson, AZ, 2000).
3. R. M. Canup, K. Righter, Eds., *Origin of the Earth and Moon* (Univ. of Arizona, Tucson, AZ, 2000).
4. S. J. Weidenschilling, J. N. Cuzzi, in *Protostars and Planets III*, E. H. Levy, J. I. Lunine, Eds. (Univ. of Arizona, Tucson, AZ, 1993), pp. 1031–1060.
5. Runaway growth, although it implies rapid growth, describes a process whereby a single dominant body grows more rapidly than the next largest bodies in the population. Typically, in a narrow accumulation zone, the final mass of the runaway embryo is two or three orders of magnitude larger than the next largest body, resulting in a bimodal mass distribution. The characteristics of runaway growth have been corroborated by several different methods; see the review by Kortenkamp *et al.* (*6*) and the recent contribution of Inaba *et al.* (*19*).
6. S. J. Kortenkamp, E. Kokubo, S. J. Weidenschilling, in (*3*), pp. 85–100.
7. R. M. Canup, C. B. Agnor, in (*3*), pp. 113–129.
8. G. Wuchterl, T. Guillot, J. J. Lissauer, in (*2*), pp. 1081–1109.
9. R. D. Mathieu, A. M. Ghez, E. L. N. Jensen, M. Simon, in (*2*), pp. 703–730.
10. A. P. Boss, *Astrophys. J. Lett.* **536**, 101 (2000).
11. I. Adachi, C. Hayashi, K. Nakazawa, *Prog. Theoret. Phys.* **56**, 1756 (1976).
12. S. J. Kortenkamp, G.W. Wetherill, *Icarus* **143**, 60 (2000).
13. F. Marzari, H. Scholl, *Astrophys. J.* **543**, 328 (2000).
14. J. Wisdom, M. Holman, *Astron. J.* **102**, 1528 (1991).
15. H. F. Levison, M. J. Duncan, *Icarus* **108**, 18 (1994).
16. R. Malhotra, *Celes. Mech. Dynamic. Astron.* **60**, 373 (1994).
17. R. Malhotra, *Nature* **365**, 819 (1993).
18. E. J. Öpik, *Proc. Irish Acad.* **54**, 165 (1951).
19. S. Inaba, H. Tanaka, K. Nakazawa, G. W. Wetherill, E. Kokubo, *Icarus* **148**, 235 (2001).
20. G. W. Wetherill, G. R. Stewart, *Icarus* **106**, 190 (1993).
21. J. E. Chambers, G. W. Wetherill, A. P. Boss, *Icarus* **119**, 261 (1996).
22. G. R. Stewart, W. M. Kaula, *Icarus* **44**, 154 (1980).
23. S. J. Kortenkamp, G. W. Wetherill, *Lunar Plan. Sci. Conf.* **31** (abstr. 1813) (2000).
24. E. Kokubo, S. Ida, *Icarus* **131**, 171 (1998).
25. D. C. Richardson, T. Quinn, J. Stadel, G. Lake, *Icarus* **143**, 45 (2000).
26. R. P. Butler *et al.*, *Astrophys. J.* **526**, 916 (1999).
27. M. C. Miller, D. P. Hamilton, *Astrophys. J.* **550**, 863 (2001).
28. Table 1 was compiled from J. Schneider's Extra-solar Planets Catalog (www.obspm.fr/encycl/catalog.html) by searching the SIMBAD database (http://simbad.u-strasbg.fr/sim-fid.pl) for the name of each star under "confirmed planets." Systems are listed in order of their Henry Draper (HD) catalog numbers with alternative names in parentheses. Some binary designations listed with SIMBAD have been questioned and may not be binaries, such as υ And (*26*). Also, some binaries are not obviously denoted in SIMBAD, such as 55 Cancri, but are described as binaries or multiples in the planet discovery papers cited in the Extra-solar Planets Catalog. One of the stars in HD168443 is a ≥17 Jupiter-mass "brown dwarf." Some binaries listed have very wide separations and may not have a direct influence on formation of terrestrial planets. Numbers in parentheses indicate that an additional planet is suspected in the system. The last two entries in the table are for the terrestrial-size pulsar planets. Millisecond pulsars are conventionally considered to have been spun-up by mass accretion from a stellar companion, which may or may not still reside in the system [although this theory has been recently questioned, see (*27*)]. The 18 systems in Table 1 include roughly 30% of the detected extrasolar planets orbiting in 60 different star systems as of 1 May 2001.

29. We are grateful to J. Chambers for the use of his *N*-body code, a recent version of which can be downloaded from http://star.arm.ac.uk/~jec/. We also thank A. Boss, D. Hamilton, and two anonymous reviewers for their helpful comments.

9 May 2001; accepted 10 July 2001

Molecular Evidence for the Early Colonization of Land by Fungi and Plants

Daniel S. Heckman,[1] David M. Geiser,[2] Brooke R. Eidell,[1] Rebecca L. Stauffer,[1] Natalie L. Kardos,[1] S. Blair Hedges[1]*

The colonization of land by eukaryotes probably was facilitated by a partnership (symbiosis) between a photosynthesizing organism (phototroph) and a fungus. However, the time when colonization occurred remains speculative. The first fossil land plants and fungi appeared 480 to 460 million years ago (Ma), whereas molecular clock estimates suggest an earlier colonization of land, about 600 Ma. Our protein sequence analyses indicate that green algae and major lineages of fungi were present 1000 Ma and that land plants appeared by 700 Ma, possibly affecting Earth's atmosphere, climate, and evolution of animals in the Precambrian.

Plants, animals, and fungi are well adapted to life on land, but the first colonists faced a harsh physical environment (*1*, *2*). The establishment of terrestrial eukaryotes may have been possible only through associations between a fungus and a phototroph (*3*, *4*). The most widespread of these symbioses today are lichens and arbuscular mycorrhizae. The former consist of cyanobacteria or green algae and ascomycotan (or more seldom, zygo- or basidiomycotan) fungi, and the latter join a plant with a glomalean fungus (*4*). It is un-

clear when land was successfully colonized by eukaryotes or how the environment was affected. However, the importance of symbiosis in this process is suggested by evidence of arbuscular mycorrhizae in the earliest fossil fungi (460 Ma) and in some of the earliest land plants (*4*–*6*). Lichens are known from the Devonian (400 Ma) (*7*), although Precambrian lichens and other fungi have been proposed (*4*, *8*). Unfortunately, most fungi and primitive plants do not preserve well in the fossil record, leaving open the possibility of an earlier, unrecorded history (*1*). Molecular clock estimates for the evolution of fungi, based on a well-studied ribosomal gene, have suggested a late Precambrian (600 Ma) colonization of land (*9*), but until now, abundant data from nuclear protein-coding genes have not been analyzed.

We assembled and aligned amino acid sequences of potentially orthologous groups from available fungi in the National Center for Biotechnology Information (GenBank) protein sequence databases (*10*). Of those, 119 proteins were found to be suitable for estimating fungal divergence times. For clustering purposes, we followed a widely used taxonomic arrangement (*11*, *12*). Molecular clock methods were used to date divergences between Basidiomycota and Ascomycota, Archiascomycetes and other Ascomycota, Hemiascomycetes and filamentous Ascomycetes, Ustilaginomycetes and Hymenomycetes, Zygomycota (Mucorales) plus Blastocladiales and Basidiomycota plus Ascomycota, and Neocallimasticales versus all other groups. We also estimated the divergence between the human pathogenic yeast *Candida albicans* and the bakers' yeast *Saccharomyces cerevisiae*, which is of importance for genetic and genomic studies of these species. The estimate between the filamentous ascomycotan groups Plectomycetes and Pyrenomycetes provides an internal time constraint within the fungal fossil record. Plectomycetes include the model fungus *Aspergillus* and many other human and animal pathogens such as *Histoplasma* and *Coccidioides*, whereas Pyrenomycetes include the model *Neurospora* and many plant pathogens such as *Fusarium* (head scab of wheat, Panama disease of banana), *Cryphonectria* (chestnut blight), and *Magnaporthe* (rice blast). Glomales, all other Zygomycota plus Blastocladiales (chytrids), and Neocallimasticales (chytrids) were recognized as monophyletic groups (*11*, *12*).

Several groups of fungi, and comparisons among groups, lacked sufficient sequences for time estimation and thus were not considered: Glomales, Urediniomycetes, and the divergences between Zygomycota (Mucorales) and Blastocladiales and between Blastocladiales and *Neocallimastix.* Because of the widespread symbiotic relationships between fungi and plants (including green algae), we also obtained divergence time estimates for a green alga (Chlorophyta, *Chlamydomonas*) versus higher plants (Embryophyta) and a moss (Bryophyta, *Physcomitrella*) versus vascular plants (Tracheophyta, *Arabidopsis*, and other taxa) (*13*). These taxa were selected because of availability of nonchloroplast nuclear protein sequences, permitting animal-based calibration.

To reduce extrapolation error, we used multiple external calibrations from older divergences among animal phyla and kingdoms (plants, animals, fungi) derived from an analysis of 75 nuclear proteins calibrated with the vertebrate fossil record (*14*, *15*). We estimated times using two methods: the multigene approach whereby times are averaged across genes (*16*, *17*) and the average-distance approach involving concatenation of distances among genes (*18*, *19*). We used a relative rate test to examine rate variation among taxa and a gamma correction to account for rate variation among sites (*20*). Rate variation was relatively low, with most comparisons averaging less than 10% difference between branches (Fig. 1). As would be expected, the branch length data for fungi, involving longer sequences (average protein length, 446 amino acids), showed less variation than branch length data for green algae and land plants, which involved shorter sequences (averaging 291 and 102 amino acids, respectively).

Divergence time estimates for nearly all

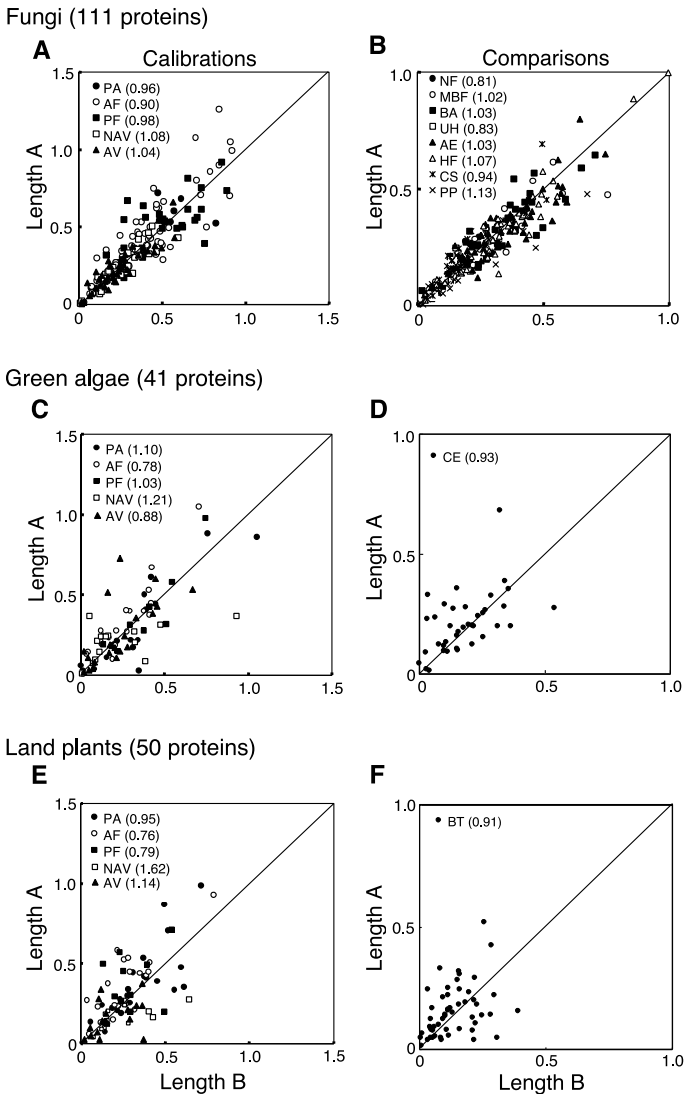

Fig. 1. Branch length differences in rate-constant proteins (those passing the relative rate test). Each datum indicates the sequence divergence (branch lengths) of two branches (A and B) compared in relative rate tests, with branch A being the first named group of each pair. The calibration pairs are plant versus animal (PA), animal versus fungi (AF), plant versus fungi (PF), nematode versus arthropod/vertebrate (NAV), and arthropod versus vertebrate (AV). (**A**) Fungi: calibrations. (**B**) Fungi: comparisons; chytrids (Neocallimasticales) versus other groups (NF), Mucorales/Blastocladiales versus Basidiomycota/Ascomycota (MBF), Basidiomycota versus Ascomycota (BA), Ustilaginomycetes versus Hymenomycetes (UH), Archiascomycetes versus other Ascomycota (AE), Hemiascomycetes versus filamentous Ascomycota (HF), *Candida albicans* versus *Saccharomyces cerevisiae* (CS), Plectomycetes versus Pyrenomycetes (PP). (**C**) Algae: calibrations. (**D**) Algae: comparisons; chlorophytan green algae versus embryophytes (higher plants) (CE). (**E**) Land plants: calibrations. (**F**) Land plants: comparisons; bryophytes (mosses) versus tracheophytes (vascular plants) (BT). Trend lines for rate constancy (slope = 1) are shown for reference. Mean branch length ratios (sum of A branches/sum of B branches) are indicated for each pair (in parentheses).

[1]Astrobiology Research Center and Department of Biology, [2]Department of Plant Pathology, Pennsylvania State University, University Park, PA 16802, USA.

*To whom correspondence should be addressed: Department of Biology, 208 Mueller Laboratory, Pennsylvania State University, University Park, PA 16802, USA; e-mail: sbh1@psu.edu

of the major divergences within fungi are deep within the Precambrian, 1458 to 966 Ma (Table 1 and Fig. 2). These times are significantly older than previous estimates based on the small-subunit nuclear ribosomal gene, which place the same splits at 660 to 370 Ma (*9*). Similarly, our dates for the *Candida-Saccharomyces* divergence (841 Ma) and the Pyrenomycetes-Plectomycetes divergence (670 Ma) are older than previous ribosomal gene estimates (140 and 310 Ma, respectively) (*9*). The closeness in divergence times of the major groups, with overlapping confidence intervals, resulted in one case of topological inconsistency: The Mucorales/Blastocladiales versus Basidiomycota/Ascomycota divergence is slightly more recent than the Basidiomycota versus Ascomycota divergence, although the difference is not significant.

Given these time estimates and assumed fungal phylogeny (*11*, *12*), we can infer that Glomales originated after chytrids diverged from the other groups, but before Basidiomycota split from Ascomycota, about 1400 to 1200 Ma. Previous estimates are 590 Ma (*9*) and 462 to 353 Ma (*21*). This corresponds to the appearance of terrestrial fungi, and pushes back the origin of the first terrestrial eukaryotes, and earliest possible mycorrhizal associations, by about 800 million years (My). These data also indicate that lineage diversification within Ascomycota and Basidiomycota began shortly after divergence of those two major groups. The green algal divergence (1061 ± 109 Ma) establishes a minimum time when green algae existed, and the bryophyte divergence (703 ± 45 Ma), between two terrestrial lineages, is a minimum molecular clock estimate for the colonization of land by plants. The latter was unexpected considering the absence of fossil land-plant spores, containing decay-resistant sporopollenin, from the Precambrian.

The more recent estimates obtained in the ribosomal RNA gene study (*9*) largely are the result of using a more recent calibration (965 Ma) for the fungi-animal divergence, based on a molecular clock estimate tied to the vertebrate fossil record (*22*). However, that calibration was revised in a subsequent study to ~1200 Ma (*23*), narrowing the difference. The calibration used here for the divergence of the three kingdoms (1576 Ma) derives from a more recent molecular clock study (*14*) also tied to the vertebrate fossil record, but based on refined vertebrate calibration dates, different methodology, and a different data set. A colonization of land by fungi deep in the Precambrian (>900 Ma) is inferred with either calibration (1200 or 1576 Ma) or data set (ribosomal RNA gene or nuclear proteins).

Because these time estimates are older than expected, it is of interest to know the effect of an internal (minimum) calibration. The oldest well-documented ascomycotan fossils are 400-My-old Rhynie chert perithecia, asci, and ascospores that resemble those of extant Pyrenomycetes (*24*). These fossils are about 60% as old as our estimate for the Plectomycetes-Pyrenomycetes divergence (670 Ma) and cannot be accounted for with the ribosomal estimate (310 Ma) (*9*). If a 60% rate adjustment is applied, the minimum times for the major fungal divergences are 875 to 580 Ma. A second fossil constraint involves red algae, which are dated to 1200 Ma (*25*). If red algae evolved on the plant lineage (*26*), the divergence of the three kingdoms (set here at 1576 Ma) (*14*) must be older than 1200 Ma. Applying this rate adjustment (76%) yields minimum time estimates of 1108 to 757 Ma for the major splits within fungi. Thus, Precambrian time esti-

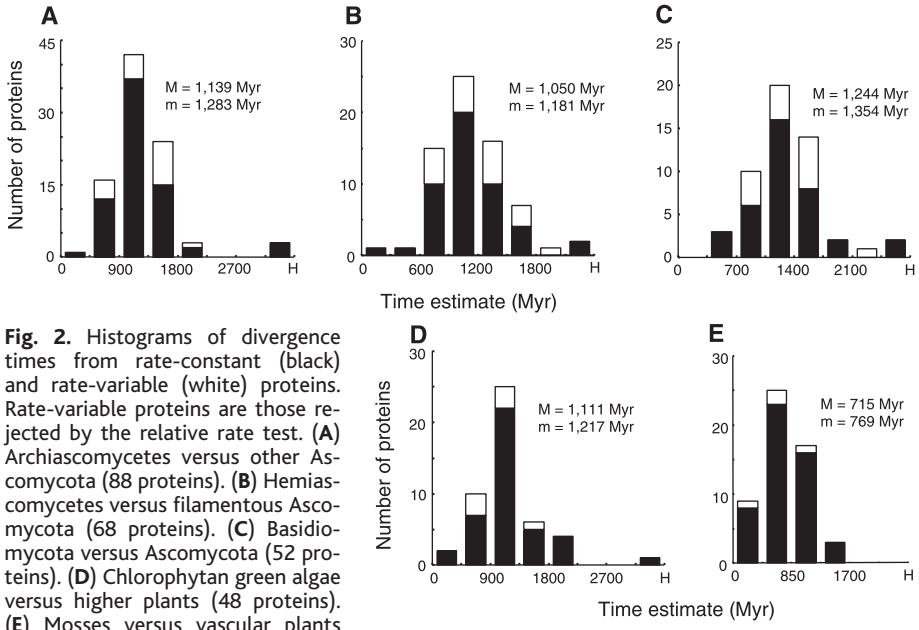

Fig. 2. Histograms of divergence times from rate-constant (black) and rate-variable (white) proteins. Rate-variable proteins are those rejected by the relative rate test. (**A**) Archiascomycetes versus other Ascomycota (88 proteins). (**B**) Hemiascomycetes versus filamentous Ascomycota (68 proteins). (**C**) Basidiomycota versus Ascomycota (52 proteins). (**D**) Chlorophytan green algae versus higher plants (48 proteins). (**E**) Mosses versus vascular plants (54 proteins). M, mode; m, mean (rate constant).

Table 1. Divergence time estimates.

Comparison	Number of proteins		Total amino acids*		Divergence time estimates (Ma)				
					Multigene		Average distance		Mean†
	All	Constant	All	Constant	All	Constant	All	Constant	(±SE)
Neocallimasticales (chytrids) vs. other groups	5	2	1,976	497	1,497	1,457	1,513	1,459	1,458 ± 70
Mucorales/Blastocladiales vs. Basidiomycota/Ascomycota	27	17	8,821	5,492	1,215	1,128	1,184	1,085	1,107 ± 56
Basidiomycota vs. Ascomycota	52	37	19,800	11,987	1,269‡	1,244‡	1,206	1,172	1,208 ± 108
Ustilaginomycetes vs. Hymenomycetes	8	4	2,948	1,301	951	982	950	950	966 ± 86
Archiascomycetes vs. other Ascomycota	88	70	37,500	27,261	1,166‡	1,139‡	1,151	1,149	1,144 ± 77
Hemiascomycetes vs. filamentous Ascomycota	68	48	26,921	17,412	1,058‡	1,050‡	1,112	1,120	1,085 ± 81
Candida albicans vs. *Saccharomyces cerevisiae*	35	26	15,258	10,763	815	837	823	844	841 ± 62
Plectomycetes vs. Pyrenomycetes	40	28	18,174	12,221	667	642	654	698	670 ± 71
Chlorophytan green algae vs. higher plants	48	41	13,996	11,541	1,099‡	1,111‡	1,010	1,010	1,061 ± 109
Mosses vs. vascular plants	54	50	5,526	5,131	708‡	715‡	680	690	703 ± 45

*Aligned, with gaps, missing data, and ambiguities removed. †Mean (multigene, constant rate; average distance, constant rate) ± SE (multigene, constant rate). ‡Mode used here.

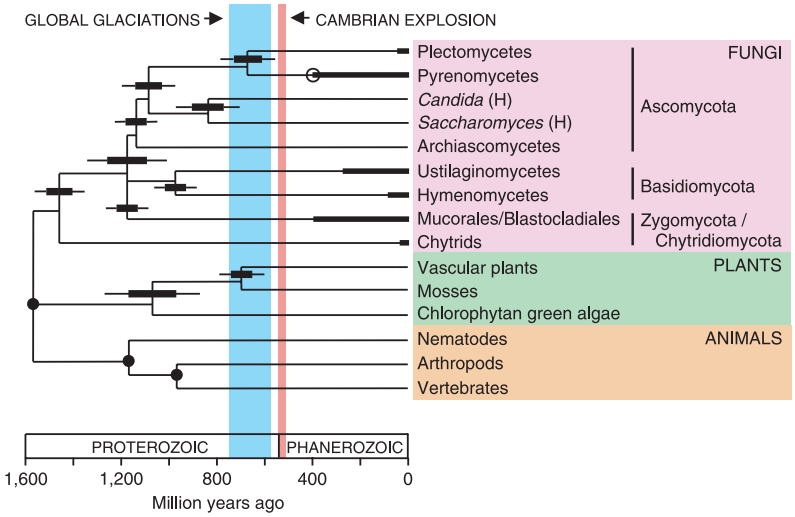

Fig. 3. Divergence time estimates for major groups of fungi, plants, and animals (Table 1). Thick horizontal bars at branch points are ±1 SE; narrow bars delimit 95% confidence intervals; thick bars on branches denote fossil record of fungi; solid circles are calibration points; open circle is internal (fungal) fossil constraint. H, Hemiascomycetes. The branching order of three groups (Ascomycota, Basidiomycota, Mucorales/Blastocladiales) is shown as unresolved for topological consistency. On the basis of branching order from other data (*11*, *12*), glomalean fungi diverged after chytrids and before the basidiomycotan/ascomycotan divergence, ~1400 to 1200 Ma.

mates also are obtained with an internal calibration and red algal fossil constraint.

Most sequence data available for timing higher plant divergences come from organellar genomes. Unfortunately, because such genomes are absent, or differ greatly, between kingdoms, it is difficult or impossible to calibrate outside of plants. Thus, calibration usually is done with the plant fossil record, especially the liverwort *Marchantia* (450 Ma) (*27*). Our time estimate of 700 Ma for the divergence of moss and vascular plants, based on external calibration and nuclear proteins, indicates that some divergences among higher plants may be older than currently thought.

One of the first steps toward the colonization of land by eukaryotes may have been the formation of a lichen symbiosis, perhaps an endosymbiosis of a fungus and a unicellular cyanobacterium (*28*). Presumably, this would have led to other symbioses between fungi and phototrophs. Lichens and free-living cyanobacteria, often with bryophytic plants, form a biological crust in harsh terrestrial environments today (*29*) and may have done so in the Neoproterozoic (900 to 544 Ma) or even earlier, perhaps along with extremophilic animals such as tardigrades.

There is geochemical evidence for terrestrial ecosystems (prokaryotic) as early as 2600 Ma (*30*) and microfossil evidence 1200 to 800 Ma (*2*). However, despite speculation of Precambrian lichens and their impact (*8*, *31*), there is no undisputed fossil evidence of terrestrial eukaryotes until the Ordovician (480 to 460 Ma), when land plants and fungi first appear (*6*, *32*). If they arose earlier, as our data suggest, their potential effect on the environment and biota should be considered. In particular, two phenomena currently explained by other mechanisms may be the result of an early colonization of land by fungi and plants. One is a period of global glaciations ("Snowball Earth" events) 750 to 580 Ma (*33*) and the other is a Neoproterozoic rise in oxygen, possibly leading to the Cambrian explosion of animals (*34*) (Fig. 3).

Fungi can enhance weathering (*31*), which in turn can lead to lower CO_2 levels and global temperatures (*33*, *35*). In addition, the burial of terrestrial carbon, rich in decay-resistant compounds of land plants (*36*) and less dependent on abundance of phosphorus (*37*), would further affect global climate. Either or both of these mechanisms could explain lower global temperatures (episodic or general) and a rise in oxygen in the Neoproterozoic. Examination of sediments from this time period with appropriate methods (*1*, *6*) may reveal fossil evidence of an early colonization of land by fungi and plants.

References and Notes

1. J. Gray, W. Shear, *Am. Sci.* **80**, 444 (1992).
2. R. J. Horodyski, L. P. Knauth, *Science* **263**, 494 (1994).
3. K. A. Pirozynski, D. W. Malloch, *Biosystems* **6**, 153 (1975).
4. M.-A. Selosse, F. LeTacon, *Trends Ecol. Evol.* **13**, 15 (1998).
5. W. Remy, T. N. Taylor, H. Hass, H. Kerp, *Proc. Natl. Acad. Sci. U.S.A.* **91**, 11841 (1994).
6. D. Redecker, R. Kodner, L. E. Graham, *Science* **289**, 1920 (2000).
7. T. N. Taylor, H. Hass, W. Remy, H. Kerp, *Nature* **378**, 244 (1995).
8. G. J. Retallack, *Paleobiology* **20**, 523 (1994).
9. M. L. Berbee, J. W. Taylor, in *The Mycota*, vol. VIIB, *Systematics and Evolution*, D. J. McLaughlin, E. McLaughlin, Eds. (Springer-Verlag, New York, 2000), pp. 229–246.
10. Sequences were aligned with Clustal W (*38*), and upon visual inspection of the alignments, highly divergent prokaryote sequences were omitted. Neighbor-joining trees were constructed from the alignments with MEGA (*39*) (complete-deletion, gamma distance), and only orthologous groups were used in subsequent analyses. Paralogous groups were identified by branching orders suggesting gene duplication, and omitted. If available, eukaryotic taxa basal to the divergence of plants, animals, and fungi were used as outgroups in rate tests. If eukaryotic sequences were unavailable, prokaryotes were used as outgroups.
11. C. J. Alexopoulos, C. W. Mims, M. Blackwell, *Introductory Mycology* (Wiley, New York, ed. 4, 1996).
12. T. Y. James, D. Porter, C. A. Leander, R. Vilgalys, J. E. Longcore, *Can. J. Bot.* **78**, 336 (2000).
13. For the green algal and bryophyte divergences, 48 proteins averaging 292 amino acids, and 54 proteins averaging 103 amino acids, respectively, were obtained for analyses. The *Physcomitrella* sequences (Leeds/Wash U. Moss EST Project) were trimmed by 10% at the 3′ end before analysis, and all alignments were checked visually to guard against expressed sequence tag (EST)–related sequence errors. Available tracheophytes were used, including *Arabidopsis*, *Brassica*, *Nicotiana*, *Oryza*, *Pisum*, *Solanum*, and *Zea*.
14. D. Y.-C. Wang, S. Kumar, S. B. Hedges, *Proc. R. Soc. London B.* **266**, 163 (1999).
15. We estimated divergence times using the animal-plant-fungus divergence (1576 Ma), the nematode-chordate and nematode-arthropod divergence (1177 Ma), and the arthropod-chordate divergence (993 Ma) as calibration points (*14*).
16. S. B. Hedges, P. H. Parker, C. G. Sibley, S. Kumar, *Nature* **381**, 226 (1996).
17. S. Kumar, S. B. Hedges, *Nature* **392**, 917 (1998).
18. M. Nei, P. Xu, G. Glazko, *Proc. Natl. Acad. Sci. U.S.A.* **98**, 2497 (2001).
19. Gene-specific rates of sequence change were estimated by linear regression (*y* intercept fixed through the origin) from one or more of these calibrations and applied to the intergroup distance estimations (*40*) to produce gene-specific time estimates. Single-gene time estimates were averaged to obtain multigene times (*16*, *17*). Where sufficient numbers of proteins (>35) were available, modes were used rather than means to reduce possible error from paralogous comparisons (*17*). For the average-distance method, time estimates were made by weighting individual gene distances and rates by sequence length, and dividing summed distances by summed rates (*18*).
20. Gene-specific gamma parameters were calculated and used for distance and time estimation (*41*). Gamma parameters averaged 1.25 and 1.19 (all genes, rate-constant genes) for the fungal alignments, 2.51 and 2.73 for the green algal alignments, and 1.58 and 1.63 for the land-plant alignments. Relative rate tests (*42*) were conducted with PHYLTEST (*40*). Analyses were performed for constant-rate genes and all genes. Sequence alignments, accession numbers, gene-specific gamma parameters, and other supplementary data are available at www.evogenomics.org/publications/data/fungi/.
21. L. Simon, J. Bousquet, R. C. Levesque, M. Lalonde, *Nature* **363**, 67 (1993).
22. R. F. Doolittle, D.-F. Feng, S. Tsang, G. Cho, E. Little, *Science* **271**, 470 (1996).
23. D.-F. Feng, G. Cho, R. F. Doolittle, *Proc. Natl. Acad. Sci. U.S.A.* **94**, 13028 (1997).
24. T. N. Taylor, H. Hass, H. Kerp, *Nature* **399**, 648 (1999).
25. N. J. Butterfield, *Paleobiology* **26**, 386 (2000).
26. D. Moreira, H. LeGuyader, H. Philippe, *Nature* **405**, 69 (2000).
27. V. V. Goremykin, S. Hansmann, W. F. Martin, *Plant Syst. Evol.* **206**, 337 (1997).
28. H. Gehrig, A. Schubler, M. Kluge, *J. Mol. Evol.* **43**, 71 (1996).
29. R. D. Evans, J. R. Johansen, *Crit. Rev. Plant Sci.* **18**, 183 (1999).
30. Y. Watanabe, J. E. J. Martini, H. Ohmoto, *Nature* **408**, 574 (2000).
31. D. Schwartzman, *Life, Temperature, and the Earth* (Columbia Univ. Press, New York, 1999).
32. P. Kenrick, P. R. Crane, *Nature* **389**, 33 (1997).

33. P. F. Hoffman, A. J. Kaufman, G. P. Halverson, D. P. Schrag, *Science* **281**, 1342 (1998).
34. A. H. Knoll, *Science* **256**, 622 (1992).
35. T. J. Crowley, R. A. Berner, *Science* **292**, 870 (2001).
36. S. Kroken, L. Graham, M. Cook, *Am. J. Bot.* **83**, 1241 (1996).
37. L. R. Kump, *Nature* **335**, 152 (1988).
38. J. D. Thompson, D. G. Higgins, T. J. Gibson, *Nucleic Acids Res.* **22**, 4673 (1994).
39. S. Kumar, K. Tamura, M. Nei, *MEGA: Molecular Evolutionary Genetic Analysis* (Pennsylvania State University, University Park, PA, 1993).
40. S. Kumar, *Phyltest: A Program for Testing Phylogenetic Hypotheses* (Institute of Molecular Evolutionary Genetics, Pennsylvania State University, University Park, PA, ed. 2.0, 1996).
41. Z. Yang, *CABIOS* (*Comput. Appl. Biosci.*) **13**, 555 (1997).
42. N. Takezaki, A. Rzhetsky, M. Nei, *Mol. Biol. Evol.* **12**, 823 (1995).

43. We thank M. Ray for assistance with data collection and L. E. Graham, J. F. Kasting, A. H. Knoll, L. R. Kump, and D. Schwartzman for comments or discussion. N.L.K. was supported by Women in Science and Engineering Research (NASA Space Grant to Penn State). Supported by grants from the NASA Astrobiology Institute (to S.B.H.).

9 April 2001; accepted 8 June 2001

Coordination of a Transcriptional Switch by HMGI(Y) Acetylation

Nikhil Munshi, Theodora Agalioti, Stavros Lomvardas, Menie Merika, Guoying Chen, Dimitris Thanos*

Dynamic control of interferon-β (IFN-β) gene expression requires the regulated assembly and disassembly of the enhanceosome, a higher-order nucleoprotein complex formed in response to virus infection. The enhanceosome activates transcription by recruiting the histone acetyltransferase proteins CREB binding protein (CBP) and p300/CBP-associated factors (PCAF)/GCN5, which, in addition to modifying histones, acetylate HMGI(Y), the architectural component required for enhanceosome assembly. We show that the accurate execution of the IFN-β transcriptional switch depends on the ordered acetylation of the high-mobility group I protein HMGI(Y) by PCAF/GCN5 and CBP, which acetylate HMGI(Y) at distinct lysine residues on endogenous promoters. Whereas acetylation of HMGI(Y) by CBP at lysine-65 destabilizes the enhanceosome, acetylation of HMGI(Y) by PCAF/GCN5 at lysine-71 potentiates transcription by stabilizing the enhanceosome and preventing acetylation by CBP.

Gene-specific transcriptional switches are thought to be generated through the dynamic assembly and disassembly of transcription factor-enhancer DNA complexes, although the mechanisms controlling these processes in real time are poorly understood. Virus-induced activation of the IFN-β gene represents one of the best characterized transcriptional switches in eukaryotic cells (*1*). A 65-bp enhancer element contains the necessary information for directing the assembly of a virus-induced enhanceosome consisting of NF-κB, IRFs, ATF-2/cJun, and the architectural protein HMGI(Y), which orchestrates this process by mediating a network of protein-DNA and protein-protein interactions (*2, 3*). The enhanceosome is assembled in the nucleosome-free enhancer region, and it activates transcription by instructing a recruitment program of chromatin-modifying activities that target a strategically positioned nucleosome masking the TATA box and start site of transcription (*4*). The first step involves recruitment of the GCN5/PCAF complex, which acetylates the nucleosome, and this is followed by recruitment of the CBP-PolII holoenzyme complex (*4–7*). Nucleosome acetylation, in turn, facilitates SWI/SNF recruitment by CBP, resulting in chromatin remodeling and binding of TFIID to the promoter (*4*).

Consistent with the observation that histone acetylation takes place at the IFN-β promoter is the fact that the histone acetyltransferase (HAT) activities of both CBP and GCN5/PCAF are required to attain maximum levels of virus-induced IFN-β transcription (*8, 9*). However, CBP and GCN5/PCAF also acetylate HMGI(Y) at distinct lysine residues (K65 and K71, respectively), causing distinct effects on transcription. Acetylation of HMGI(Y) by CBP decreases its affinity for DNA, resulting in enhanceosome destabilization and transcriptional shutoff (*8*). Here, we show that acetylation of HMGI(Y) by GCN5/PCAF strengthens enhanceosome assembly and protects the enhanceosome from premature disruption by CBP-dependent acetylation of HMGI(Y).

To examine the role of K71 acetylation, an HMGI(Y) derivative in which K71 was mutated to arginine was used in cotransfection experiments along with an IFN-β reporter plasmid with or without a PCAF or PCAF HAT$^-$ expression vector (*10*). These experiments revealed that expression of the mutant HMGI(Y) with or without the PCAF expression vectors strongly reduced the levels of virus-induced transcription throughout the time course, especially at early time points (e.g., 9 hours), and thus suggested a link between PCAF HAT activity and HMGI(Y) acetylation at K71, in addition to the link between PCAF HAT activity, histone acetylation, and IFN-β gene expression (*4, 10*). Therefore, because acetylation of HMGI(Y) by PCAF does not alter the affinity of HMGI(Y) for DNA (*8*) and because K71 lies in one of the critical protein-protein interaction domains of HMGI(Y) (*3*), we tested the effect of PCAF acetylation on the ability of HMGI(Y) to interact with the IFN-β activators. Recombinant wild-type (WT) or mutant HMGI(Y) proteins were radiolabeled by acetylation using PCAF or CBP in the presence of ^{3}H-labeled acetyl-CoA, and the resulting mixture of ^{3}H-labeled (~10 to 20%) and nonlabeled HMGI(Y) proteins was tested for interaction with the activators by glutathione *S*-transferase (GST) interaction experiments (*11*). Fluorography revealed that the fraction of HMGI(Y) protein radiolabeled by PCAF acetylation, but not by CBP acetylation, preferentially interacted with all activators (Fig. 1A, compare lanes 1 through 5 with 6 through 10). Parallel Western blot analysis revealed that CBP-acetylated HMGI(Y) interacted with the activators as efficiently as the unacetylated protein (Fig. 1A, lanes 22 through 33), thus ruling out the possibility that HMGI(Y) acetylation by CBP decreases its affinity for the activators. In addition, PCAF-acetylated and ^{3}H-labeled HMGI(Y)(K71R) did not preferentially interact with the activators (Fig. 1A, lanes 11 through 15), although PCAF-acetylated ^{3}H-labeled HMGI(Y) (K65R) interacted with the activators as efficiently as PCAF-acetylated wild-type HMGI(Y) (Fig. 1A, compare lanes 1 through 5 with 16 through 21).

To further support the conclusions from these experiments, three peptides were synthesized that encompassed the protein-protein interaction domain of HMGI(Y) but differed only in their acetylation state (Fig. 1B). These peptides were tested for their ability to compete with in vitro translated ^{35}S-labeled HMGI(Y) for interaction with p50 (*11*). Whereas neither the unacetylated nor the K65-acetylated peptide could significantly compete with HMGI(Y) for interaction with p50 at these concentrations (Fig. 1C, lanes 1

Department of Biochemistry and Molecular Biophysics, Columbia University, 630 West 168th Street, New York, NY 10032, USA.

*To whom correspondence should be addressed. E-mail: dt73@columbia.edu